

Article

The Role of Impregnated Sodium Ions in Cu/SSZ-13 NH₃-SCR Catalysts

Chen Wang ¹ , Jun Wang ², Jianqiang Wang ², Zhixin Wang ², Zexiang Chen ², Xiaolan Li ¹, Meiqing Shen ^{2,*}, Wenjun Yan ³ and Xue Kang ^{4,*}

¹ School of Environment and safety Engineering, North University of China, Taiyuan 030051, China; chenwang87@nuc.edu.cn (C.W.); lxldmu@163.com (X.L.)

² Key Laboratory for Green Chemical Technology of State Education Ministry, School of Chemical Engineering & Technology, Tianjin University, Tianjin 300072, China; wangjun@tju.edu.cn (J.W.); jianqiangwang@tju.edu.cn (J.W.); wangzhixin@tju.edu.cn (Z.W.); tjuczx@tju.edu.cn (Z.C.)

³ Analytical Instrumentation Center, Institute of Coal Chemistry, Chinese Academy of Sciences, Taiyuan 030001, China; yanwenjun@sxicc.ac.cn

⁴ School of Chemical Engineering and Technology, North University of China, Taiyuan 030051, China

* Correspondence: mqshen@tju.edu.cn (M.S.); kx19871111@tju.edu.cn (X.K.); Tel.: +86-155-3689-0402 (X.K.)

Received: 30 October 2018; Accepted: 27 November 2018; Published: 30 November 2018



Abstract: To reveal the role of impregnated sodium (Na) ions in Cu/SSZ-13 catalysts, Cu/SSZ-13 catalysts with four Na-loading contents were prepared using an incipient wetness impregnation method and hydrothermally treated at 600 °C for 16 h. The physicochemical property and selective catalytic reduction (SCR) activity of these catalysts were studied to probe the deactivation mechanism. The impregnated Na exists as Na⁺ on catalysts and results in the loss of both Brønsted acid sites and Cu²⁺ ions. Moreover, the high loading of Na ions destroy the framework structure of Cu/SSZ-13 and forms new phases (SiO₂/NaSiO₃ and amorphous species) when Na loading was higher than 1.0 mmol/g. The decreased Cu²⁺ ions finally transformed into Cu_xO, CuO, and CuAlO_x species. The inferior SCR activity of Na impregnated catalysts was mainly due to the reduced contents of Cu²⁺ ions at kinetic temperature region. The reduction in the amount of acid sites and Cu²⁺ ions, as well as copper oxide species (Cu_xO and CuO) formation, led to low SCR performance at high temperature. Our study also revealed that the existing problem of the Na ions' effect should be well-considered, especially at high hydrothermal aging when diesel particulate filter (DPF) is applied in upstream of the SCR applications.

Keywords: Cu/SSZ-13; NH₃-SCR; sodium ions; deactivation mechanism

1. Introduction

So far, selective catalytic reduction of NO_x with ammonia (NH₃-SCR) has been proved to be the most excellent post-processing technique for lean NO_x control in diesel vehicle emissions. Cu/SSZ-13, one of the chabazite (CHA) zeolites with a simple topological structure, receives a lot of attention because it provides the opportunity to understand the SCR mechanism of zeolites [1]. Besides, compared with other commercial zeolites, such as ZSM-5 and BEA, Cu/SSZ-13 catalysts with outstanding NH₃-SCR performance and hydrothermal stability are suitable for selection as a good candidate to meet the China VI emission regulation [2–8].

Sodium (Na) ions, one type of alkali ions, usually comes from urea solution, bio-diesel fuel, and aerosol particulates. Since Na can exchange with acid sites on NH₃-SCR catalysts, the Na effect has been recognized as a non-negligible problem in NH₃-SCR catalysts. For Cu/SAPO-34 catalysts, Ma et al. [9] found the NH₃-SCR activity of Cu/SAPO-34 was greatly reduced at a high content of alkali

(>0.5%) mainly due to the decreased amount of isolated Cu^{2+} formed CuO_x clusters. Wang et al. [10] further found that alkali decreased the number of Brønsted acid sites and NH_3 coverage, and would decrease the SCR reaction rate. In our previous study [11], the different contents of Na impact on Cu/SAPO-34 were also studied. Except for the decrease of active sites and acidity, the results also showed the framework of Cu/SAPO-34 damaged and CuAlO_x species formed at a high content of sodium (>0.8%), and all these factors hindered the SCR activity.

In recent years, some studies have also considered the Na ions' effect on Cu/SSZ-13 catalysts, but most of them focused on co-cation Na ions. Gao et al. [12] investigated the effects of co-cation Na on Cu/SSZ-13 catalyst. They found $\approx 1.78\%$ Na promoted SCR performance at low temperatures and helped to improve the hydrothermal stability of Cu/SSZ-13 because Na ions modified the redox of active sites and protected the framework of CHA structure. Zhao et al. [13] found a high amount of co-cation Na ions decreased the hydrothermal stability of Al-rich Cu/SSZ-13 at 750 °C for 5 h because the excess amount of Na ions weakened the interaction between Cu ions and the zeolitic framework and formed Cu_xO species. Xie et al. [14] found one-pot-synthesized Cu/SSZ-13 with higher co-cation Na contents showed poorer hydrothermal stability at 750 °C for 16 h, which was attributed to Cu species with poor stability and CHA structure deterioration. Even though some achievements have been made on co-cation Na, the conclusion could not be applied in real-world applications because co-cation Na ions have already existed before Cu exchange and could not represent the deposition of Na in the real-world. As far as we know, few studies have investigated the effect of impregnated Na on Cu/SSZ-13 catalysts. Fan et al. [15] studied the impregnated alkali and alkaline metal effect on Cu/SSZ-13 after hydrothermal aging. They found less of a decrease of SCR activity in 0.5 mmol/g Na-impregnated samples compared with fresh Cu/SSZ-13 when samples were hydrothermally treated at 700 °C for 12 h. However, the tolerance to Na ions and the overall influence could not be obtained because only one impregnated sample was shown. Therefore, the effect of impregnated Na on Cu/SSZ-13 should be further studied.

In combination with conclusions made on Na impregnated Cu/SAPO-34 catalysts, in this study, the following key points about the Na effect on Cu/SSZ-13 should be carefully considered: (1) whether Na ions affect SCR performance, (2) whether Na ions damage the framework of Cu/SSZ-13, and (3) whether other copper species except for Cu_xO will form. In order to probe its nature, four different Na metal loading samples with 0.3, 0.5, 1.0, and 1.5 mmol/g (Na/Al = 0.23, 0.38, 0.77, and 1.15) were obtained using an incipient wetness impregnation method and were hydrothermally treated under the relative lower temperature at 600 °C for 16 h. Through characterizations with Brunauer–Emmett–Teller measurements (BET), X-ray diffraction (XRD), and nuclear magnetic resonance (NMR), the change law of the framework of Cu/SSZ-13 catalysts upon hydrothermal aging was revealed. NH_3 -TPD and Ex-situ diffuse reflectance infrared Fourier transform spectra (ex situ DRIFTS) were used to investigate the acidity variation. The nature of copper species changing was acquired using H_2 temperature-programmed reduction (H_2 -TPR), electron paramagnetic resonance (EPR), and UV-Visible diffuse reflectance spectra (UV-Vis DRS spectra). Furthermore, the existing state of Na over Cu/SSZ-13 catalysts had been studied using CO_2 -DRIFTS measurements.

2. Results

2.1. Structural Characterization

2.1.1. BET and XRD Results

To probe the effect of Na ions on catalysts after 600 °C hydrothermal treatment, all catalysts were first measured using BET and the results are shown in Table 1. The reduction of the surface area of the Na-impregnated samples shows a strong relation with the amount of Na introduced into catalysts. When F-Cu went through a low content Na impregnation treatment, a lower reduction of surface area was found on Na-Cu-0.3 and Na-Cu-1.5. Meanwhile, the high contents of Na impregnation led to

an obvious decline in the BET surface area, where a reduction of 25.3% and 65% were observed on Na-Cu-1.0 and Na-Cu-1.5, respectively, compared with F-Cu.

Table 1. Na contents and BET surface area of fresh and Na impregnated catalysts.

Samples' Name	Na Contents (%) ¹	BET Surface Area	ΔS (%) ²
F-Cu	0	792	—
Na-Cu-0.3	0.7	747	5.6
Na-Cu-0.5	1.2	737	6.9
Na-Cu-1.0	2.3	591	25.3
Na-Cu-1.5	3.5	277	65.0

$$^1 \text{ Na contents measured using ICP-AES; } ^2 \Delta S(\%) = \frac{S_{\text{F-Cu}} - S_{\text{Na-Cu-x}}}{S_{\text{F-Cu}}} \times 100\%.$$

To further investigate the impact of introduced Na ions on the Cu/SSZ-13 catalyst, XRD experiments were performed. As shown in Figure 1a, the diffraction peaks of the chabazite phase ($2\theta = 9.6^\circ, 13^\circ, 16.3^\circ, 18.0^\circ, 20.9^\circ,$ and 25.3°) can be observed in fresh and Na introduced catalysts, illustrating that all catalysts had the typical chabazite (CHA) structure [16,17]. Figure 1b shows the relative crystallinity of different catalysts. The detailed calculation method of the relative crystallinity of catalysts are found in our previous study [11]. The 4%, 10%, 28%, and 56% reduction in crystallinity were found for Na-Cu-0.3, Na-Cu-0.5, Na-Cu-1.0, and Na-Cu-1.5, respectively, compared with F-Cu. The changing trend of the relative crystallinity was consistent with the BET results. It can be concluded that the decrease of BET surface area was due to the declined structure integrity of Cu/SSZ-13. Notably, the diffraction peak centered at 21.63° assigned to SiO_2 or NaSiO_3 crystalline appeared on Na-Cu-1.0 and Na-Cu-1.5 [11,18], which also suggests that the CHA structure was no longer intact. The intensity of this new peak became more intense with an increased Na amount. Besides that, some amorphous phases were also observed in Na-Cu-1.5 because the baseline of XRD pattern was non-horizontal between 18° and 25° .

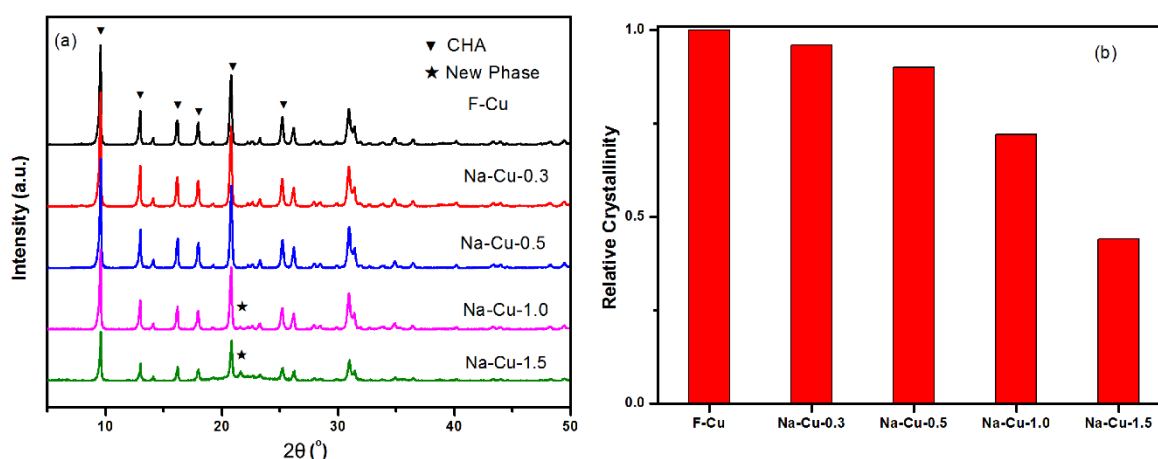


Figure 1. XRD pattern (a) and relative crystallinity (b) of fresh and Na-impregnated catalysts.

2.1.2. NH_3 -TPD Results

Figure 2a shows the NH_3 -TPD results of fresh and Na introduced Cu/SSZ-13 catalysts. For fresh Cu/SSZ-13, two peaks centered at $\approx 250^\circ\text{C}$ (peak A) and $\approx 420^\circ\text{C}$ (peak B) can be observed. In order to identify the different acid sites, DRIFTS experiments were conducted on F-Cu with stepwise NH_3 adsorption with increasing temperature (Figure S1). The desorption peak at $\approx 250^\circ\text{C}$ (peak A) was considered to be NH_3 desorbed on Lewis acid sites (Cu^{2+} ions) and the high-temperature desorption peak centered at $\approx 420^\circ\text{C}$ (peak B) was assigned to NH_3 released from Brønsted acid sites (Si-O(H)-Al). For Na-impregnated catalysts, another peak centered at 190°C (peak C) appeared.

The new peak should be assigned to NH_3 desorbed from Na^+ sites, which was consistent with the result of Gao's study [12].

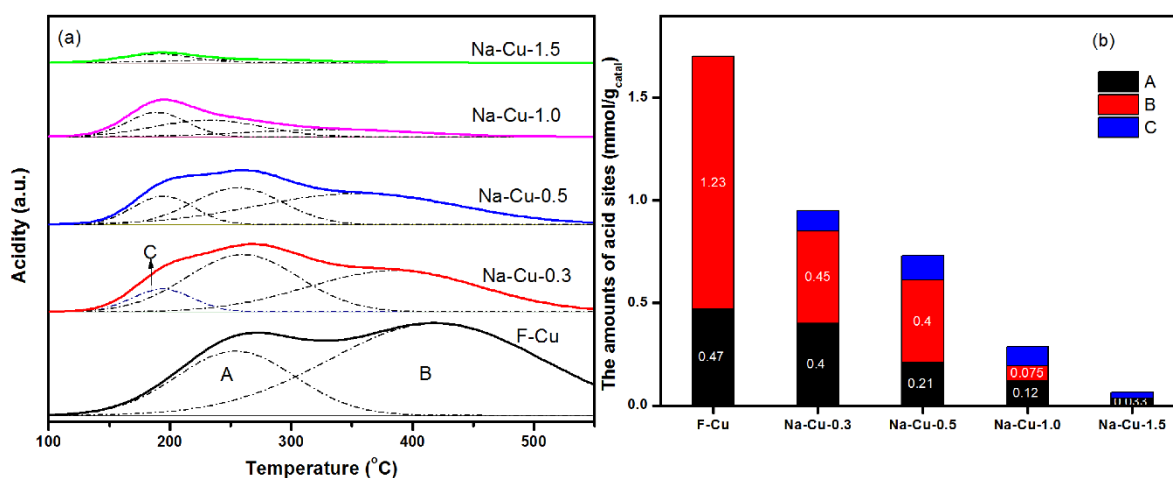


Figure 2. NH_3 -TPD results (a) and acidity (b) of fresh and Na-impregnated catalysts. The reaction was carried out with a feed containing 500 ppm NH_3 , balance N_2 , and with GHSV = 80,000 h^{-1} .

Figure 2b shows the acid contents of different catalysts. The fresh Cu/SSZ-13 showed the highest acidity among all catalysts. After the Na-impregnation process, the acidity declined and the reduction degree rose with increase amounts of introduced Na. When the Na loading reached 0.3 mmol/g, the desorption peak B assigned to Si-O(H)-Al bonds mainly decreased. Then, peak A, attributed to Cu^{2+} ions, declined when the Na loading was higher than 0.3 mmol/g. The total acidity decreased in the following order: F-Cu (1.7 mmol/g) > Na-Cu-0.3 (0.95 mmol/g) > Na-Cu-0.5 (0.73 mmol/g) > Na-Cu-1.0 (0.29 mmol/g) > Na-Cu-1.5 (0.06 mmol/g).

2.1.3. Ex Situ DRIFTS Results

Figure 3 shows the ex situ DRIFTS results of the fresh sample with those of Na-impregnated ones. The IR bands in the 3500–3800 cm^{-1} region were related to the stretching vibration modes of OH groups (–OH) [2,12,19]. IR bands at 3733 cm^{-1} corresponded to isolated silanols (SiOH) and at 3655 cm^{-1} to $[\text{Cu}(\text{OH})]^+$ [2]. Two strong bands at 3604 and 3580 cm^{-1} were assigned to the Brønsted OH groups as (Si-O(H)-Al) [2,12,19]. Moreover, the 1000–800 cm^{-1} region in the IR corresponded to a framework T–O–T vibration that was perturbed by the presence of exchanged Cu ions. The bands at 950 and 900 cm^{-1} were associated with an internal asymmetric framework vibration perturbed by two types of copper cations ($[\text{Cu}(\text{OH})]^+$ in 8 MR and Cu^{2+} in 6 MR) [5,20,21].

For the fresh and Na impregnated catalysts, the introduction of Na reduced the intensity of Brønsted OH groups and exchanged Cu ions over Cu/SSZ-13. Furthermore, the IR band intensity of these groups showed a downward trend with the amount of Na increasing (from 0.3 mmol/g to 1.5 mmol/g).

2.1.4. CO_2 -DRIFTS Results

To probe the Na existing state, CO_2 -DRIFTS tests were performed, and the results are shown in Figure 4. Two IR bands at 2354 and 2346 cm^{-1} were assigned to the vibrations of CO_2 interacting with Na^+ ions on exchange sites on catalysts [11].

When Na was introduced in Cu/SSZ-13 catalysts, two IR bands appeared indicating Na existed as an ionic state on Si-O(Na^+)-Al.

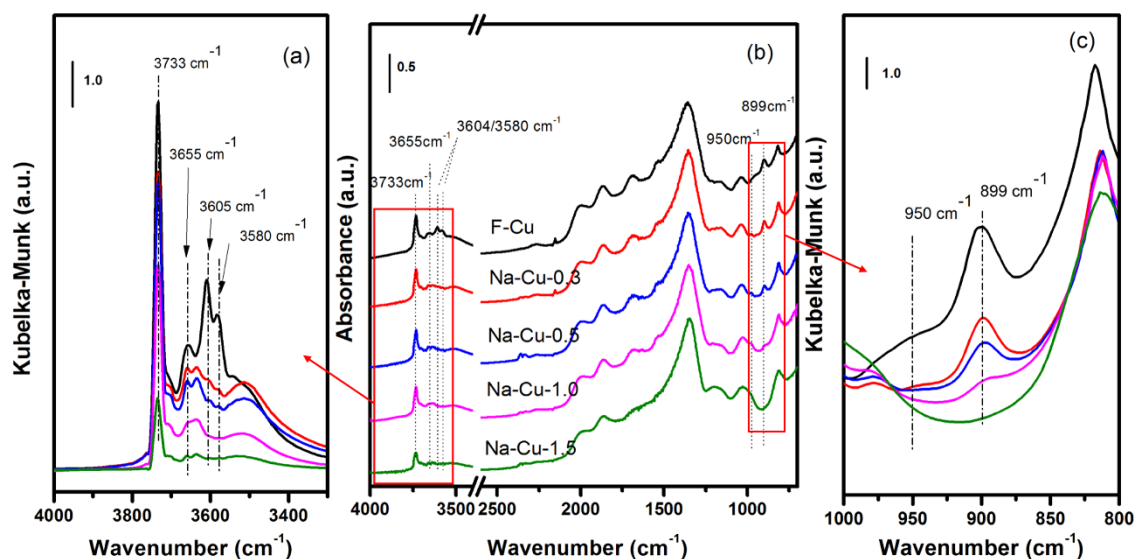


Figure 3. Ex situ DRIFTS results of fresh and Na-impregnated catalysts. Ex situ DRIFTS results between 4000 and 3300 cm^{-1} , units in Kubelka-Munk (a); ex situ DRIFTS results between 4000 and 800 cm^{-1} , units in absorbance (b); ex situ DRIFT spectra between 1000 and 800 cm^{-1} , units in Kubelka-Munk (c).

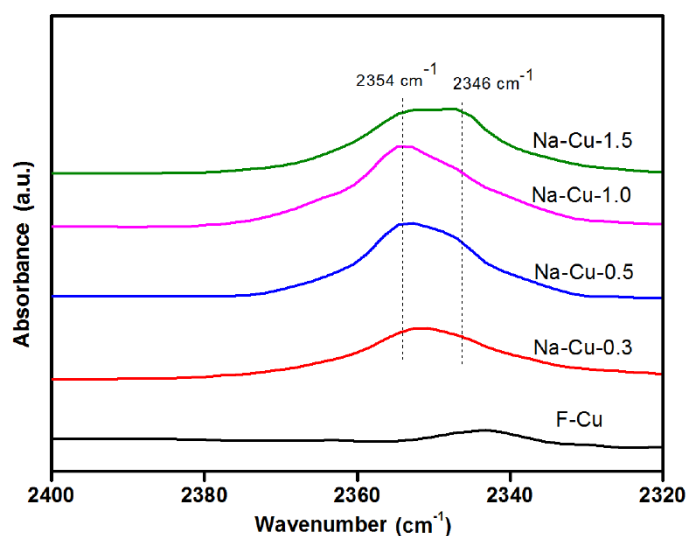


Figure 4. CO_2 -DRIFTS results of fresh and Na-impregnated catalysts.

2.2. Copper Species Variation on Cu/SSZ-13

Since Cu species bring high NH_3 -SCR performance, the variation of copper species affected by Na introducing should be considered. Thus, in this part, the overall change regulation of Cu species is qualitatively and quantitatively measured.

2.2.1. EPR Results

Since other copper state and oxidation species are EPR silent [22], EPR is a sensitive method to measure the amount of $[\text{Cu}(\text{OH})]^+$ in 8 MR and Cu^{2+} in 6 MR using hydrated catalysts [3,22]. Figure 5a shows the EPR spectra of the fresh and Na introduced Cu/SSZ-13 catalysts. All Na-impregnated catalysts showed the same coordination environment as the F-Cu with $g// = 2.39$ and $A// = 136$ G, which is consistent with other studies [23]. Meanwhile, another new hyperfine splitting over Na-Cu-1.5 ($g// = 2.32$ and $A// = 147$ G) was observed, and a new feature was also found at 3310 G on Na-Cu-1.5, which was attributed to the CuAlO_x species [11,24,25].

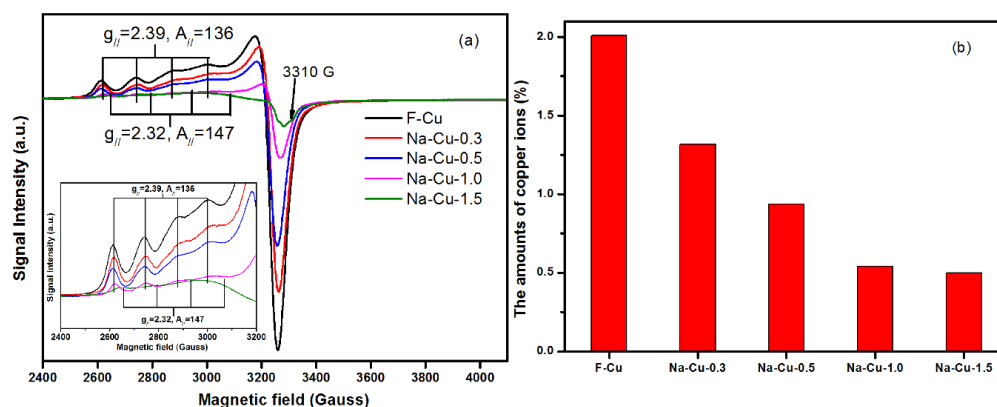


Figure 5. EPR spectra (a) and the quantitative results (b) of fresh and Na-impregnated catalysts.

Figure 5b compares the number of Cu^{2+} ions on the Na impregnated Cu/SSZ-13 catalysts from EPR spectra using the standard CuSO_4 solution as a reference. The number of Cu^{2+} ions decreased in the following order: F-Cu (2.01%) > Na-Cu-0.3 (1.32%) > Na-Cu-0.5 (0.94%) > Na-Cu-1.0 (0.54%) > Na-Cu-1.5 (0.50%). Notably, since Cu^{2+} ions in CuAlO_x species have an EPR signal [11,24,25], the number of Cu^{2+} ions over Na-Cu-1.5 contained both the amounts of Cu^{2+} ions left and Cu^{2+} in CuAlO_x species.

2.2.2. H_2 -TPR Results

H_2 -TPR measurement is a common method to get the variation of all reducible copper species, thus the fresh and Na impregnated catalysts were measured and the results are shown in Figure 6a. For the fresh sample, two peaks centered at $\approx 220^\circ\text{C}$ and $\approx 350^\circ\text{C}$ represent the reduction of $[\text{Cu}(\text{OH})]^+$ in the CHA cages to Cu^+ and the reduction of Cu^{2+} near 6 MR to Cu^+ , respectively [5,26–28]. Another peak centered at $280\text{--}300^\circ\text{C}$ was present for the Na impregnated catalysts, which was assigned to the reduction of copper oxides species to Cu^0 [6,26]. Meanwhile, the reduction peak at $\approx 410^\circ\text{C}$, which was attributed to the reduction of CuAlO_x species, is shown for Na-Cu-1.5 [13,29,30].

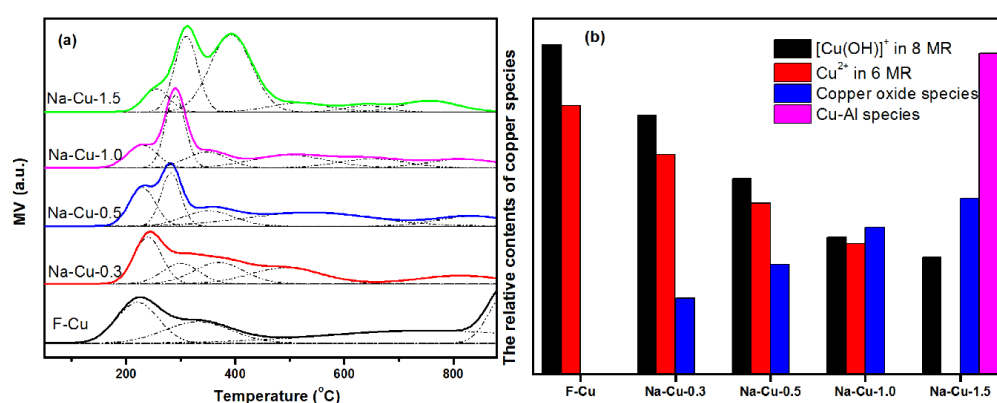


Figure 6. H_2 -TPR results (a) and qualitative results (b) of fresh and Na-impregnated catalysts.

Figure 6b shows the relative contents of the different copper species from the H_2 -TPR results. The amounts of Cu^{2+} declined with an increase in Na loading, while copper oxide species contents increased. Besides, the CuAlO_x species appeared on Na-Cu-1.5, which is consistent with our EPR results shown in Figure 5.

2.2.3. UV-Vis DRS Results

To further prove the variation of different Cu species amounts on catalysts, UV-Vis DRS spectra, a qualitative generic analysis method, was used and the results are shown in Figure 7. The band

centered at 205 nm was assigned to the oxygen-to-metal charge transfer related to Cu^{2+} ions [9,15]. The 300–600 nm region was attributed to transitions in Cu_xO , such as charge transfer transitions in O–Cu–O and Cu–O–Cu [4,31]. In addition, the region between 600 and 800 nm was assigned to the electron d–d transitions of Cu^{2+} in distorted octahedral surrounding by oxygen in CuO particles [9,15].

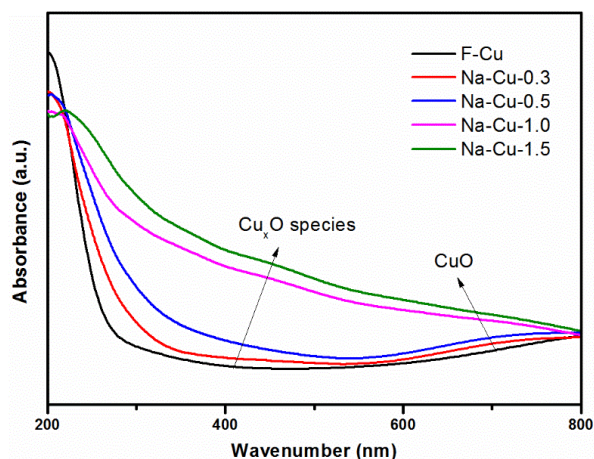


Figure 7. UV-Vis DRS results of fresh and Na-impregnated catalysts.

In general, the intensity of band at 205 nm, assigned to Cu^{2+} ions, declined when Na content increased in the Cu/SSZ-13. Meanwhile, the intensity of the regions attributed to Cu_xO (300–600 nm) and CuO (600–800 nm) increased as Na contents rose.

2.3. NH_3 -SCR Reactions over Cu/SSZ-13

2.3.1. NH_3 -SCR Activity

Figure 8a shows the NH_3 -SCR reaction of fresh and Na-impregnated Cu/SSZ-13 catalysts. Compared to F-Cu, the NO_x conversion of Na-impregnated catalysts declined with the increase in Na loading. Na-Cu-1.5 was the least active catalyst among all the samples over the whole temperature region. In addition, the N_2O formation should also be considered. The highest N_2O formation was found on the fresh catalysts at 250 °C (5 ppm). While, compared with F-Cu, the Na-introduced catalysts decreases the N_2O formation by 1 to 4 ppm at 250 °C and increased the N_2O concentration by 1 to 3 ppm at high temperatures (Figure 8b).

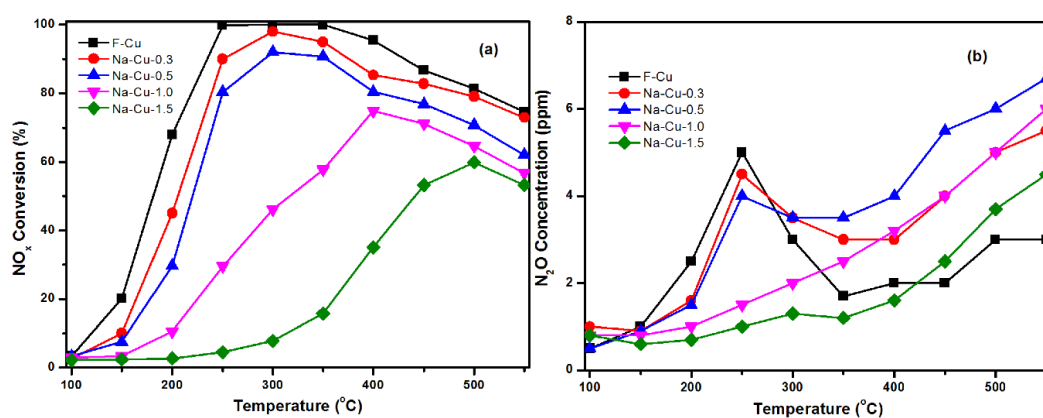


Figure 8. (a) NO_x conversion as a function of reaction temperature over catalysts; (b) N_2O formation during NH_3 -SCR reaction on the catalysts (b). The reaction was carried out with a feed containing 500 ppm NO_x , 500 ppm NH_3 , 10% O_2 , 3% H_2O , balance N_2 , and with GHSV = 80,000 h^{-1} .

2.3.2. Activation Energy (Ea) Measurements

Figure 9 shows the Arrhenius plots for the SCR reaction over the fresh and Na-impregnated catalysts and all kinetic measurements were taken at <20% NO_x conversion. It is clearly seen that the SCR reaction rate decreased with an increase of Na intake. Moreover, the apparent activation energies (E_a) change with different catalysts. All samples, except for Na-Cu-1.5, had similar E_a (E_a = 62 ± 2 kJ/mol); meanwhile, the E_a value of Na-Cu-1.5 was considerably lower (E_a = 28.5 kJ/mol).

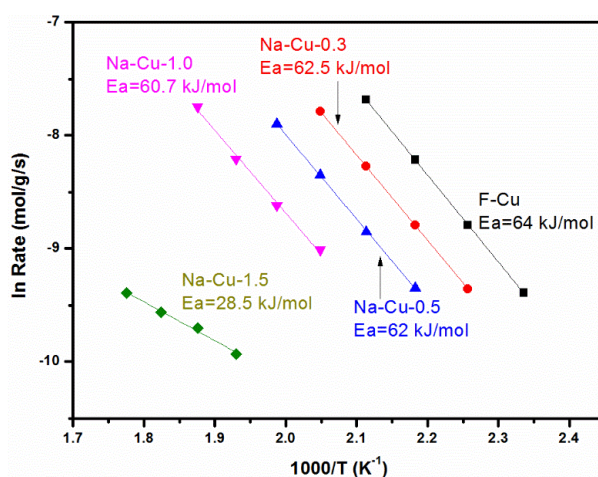


Figure 9. Arrhenius plots of the SCR reaction rates over fresh and Na-impregnated catalysts. The reaction was carried out with a feed containing 500 ppm NO_x, 500 ppm NH₃, 10% O₂, 3% H₂O, balance N₂, and with GHSV = 316,800 h⁻¹.

3. Discussion

3.1. Effect of Na Ions on CHA Structure over Cu/SSZ-13

For Na impregnated catalysts with lower Na loadings (Na-Cu-0.3 and Na-Cu-0.5), the Na content had little impact on the CHA structure integrity because of the slight reduction of surface area and relative F-Cu crystallinity according to our BET and XRD results (Table 1 and Figure 1). Even though the CHA structure was intact, the acid sites, including Brønsted acid sites and Cu²⁺ ions, declined with an increase of Na amounts, as shown in our NH₃-TPD and ex situ DRIFTS results (Figures 2 and 3). This was induced by impregnated Na, which decreased acidity and exchanged the acid sites on Cu/SSZ-13 during post-treatment, as proved via CO₂-DRIFTS results (Figure 4). The surface area and relative crystallinity decreased significantly when Na loadings were greater than 2% in catalysts (Na-Cu-1.0 and Na-Cu-1.5). Moreover, SiO₂/NaSiO₃ and amorphous species formed, illustrating that the CHA structure of Cu/SSZ-13 was destroyed by high contents of Na. This is consistent with our previous study on Na impregnated Cu/SAPO-34 [11]. As a result, a greater exchange process, as well as the CHA structure damage with high Na intake, was owed to the inferior acidity and low intensity of acid sites compared with other samples (Figures 2 and 3).

To comprehend the effect of Na ions on the CHA structure, the chemical environment of ²⁹Si and ²⁷Al on Na-Cu-1.0 and Na-Cu-1.5 were compared to those of F-Cu in Figure 10. F-Cu, the fresh catalyst, presented two framework Si features, assigned to Si(3Si, 1Al) and Si(4Si, 0Al), at -105 and -111 ppm, respectively, as well as one framework Al feature at 57.5 ppm [3]. However, the spectroscopy pattern changed when Na loading increased up to 1.5 mmol/g (Na-Cu-1.5). The peak of ²⁹Si NMR spectra became broad due to the breakage of Si-O-Al bonds and formation of amorphous silicon complexes, which resulted in the non-horizontal baseline XRD pattern of Na-Cu-1.5 [32]. Meanwhile, the ²⁷Al NMR spectrum (Figure 10b) shows non-framework Al centered at -36.5 ppm [13], which illustrates the dealumination process and broken Si-O-Al bonds.

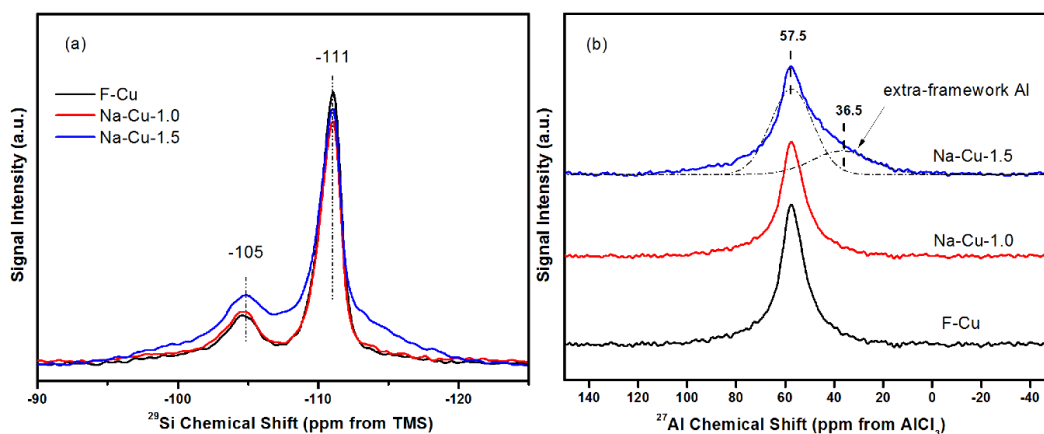


Figure 10. (a) ^{29}Si NMR and (b) ^{27}Al NMR spectra of F-Cu, Na-Cu-1.0, and Na-Cu-1.5.

Hydrothermal stability is an essential issue for Cu/SSZ-13 catalysts. It is interesting to note that the chemical environment of Al and Si did not change over Cu/SSZ-13 with hydrothermal treatment at 600 °C. However, the framework of Cu/SSZ-13 was damaged when Na loading was higher than 1.0 mmol/g, as shown in our XRD and NMR results (Figures 1 and 10). The results suggest high Na loading is not beneficial for Cu/SSZ-13 stability against hydrothermal aging. Furthermore, the impact of low Na loading on hydrothermal stability of Cu/SSZ-13 was studied by hydrothermally aging Na-Cu-0.3 at 750 °C for 16 h in air containing 10% water vapor. According to the XRD results in Figure S2, low Na contents also damaged the CHA structure and formed $\text{SiO}_2/\text{NaSiO}_3$, revealing the stability reduced when the hydrothermal temperature increased. In conclusion, the impregnated Na reduced the hydrothermal stability of Cu/SSZ-13, especially at high temperatures when DPF was applied upstream of the SCR applications.

3.2. Effect of Na Ions on Acid Sites over Cu/SSZ-13

H_2 -TPR results show that two reduction peaks (≈ 220 °C and ≈ 350 °C) were assigned to two different types of Cu^{2+} ions present on F-Cu, which suggests the state of copper species on fresh catalysts was an ionic state. The similar content of copper loading obtained using EPR and ICP results (2.01% vs 1.91%) also confirmed this suggestion. When Na was introduced to Cu/SSZ-13 catalysts, Na competitively took over the exchange sites and influenced the distribution and amounts of acid sites, including Brönsted acid sites and Cu^{2+} ions. Our NH_3 -TPD and ex situ DRIFTS results (Figures 2 and 3) showed that Na intakes reduced the both amounts of Brönsted acid sites and Cu^{2+} ions. Moreover, Brönsted acid sites reduced more than that of Cu^{2+} based on a greater decrease of desorption peak B and the intensity of bands (3604 and 3580 cm^{-1}) as shown in Figures 2 and 3. The results show that Na could easily exchange with H ions (Si-O(H)-Al) rather than Cu^{2+} ions on Cu/SSZ-13 due to the stronger acidity of H ions [11].

The change processes of Cu^{2+} ions contents and distributions could be monitored using H_2 -TPR results (Figure 6). The amounts of both types of Cu^{2+} ions, $[\text{Cu(OH)}]^+$ in 8 MR and Cu^{2+} in 6 MR, decreased when Na loading increased to 1.0 mmol/g, and Cu^{2+} in 6 MR completely disappeared when Na contents reached up to 1.5 mmol/g. Based on the results of ex situ DRIFTS, the regulation of Cu^{2+} ions changed: the intensity of both $[\text{Cu(OH)}]^+$ (3655 cm^{-1}) and Cu^{2+} (900 cm^{-1}) declined at the initial stage when Na impregnated and only the weak intensity of $[\text{Cu(OH)}]^+$ was left on Na-Cu-1.5 (Figure 3). In addition, the property of Cu^{2+} ions on catalysts was also confirmed using EPR and H_2 -TPR results (Figures 5 and 6). Since all catalysts had the same hyperfine splitting with $g// = 2.39$ and $A// = 136$ G, as well as a similar reduction peak, the property of the left Cu^{2+} ions was not affected by Na. All results showed that Na impregnation influenced the Cu^{2+} ions amount, but had no effect on the remaining Cu^{2+} ions. Moreover, Cu_xO and CuO present on all Na-impregnated catalysts and their contents increased with increasing Na loading as shown in the H_2 -TPR and UV-Vis DRS

results (Figures 6 and 7). Note that on Na-Cu-1.5, besides Cu_xO and CuO , CuAlO_x species formed a new hyperfine splitting ($g// = 2.32$, $A// = 147$ G), and showed a reduction peak at ≈ 410 °C in the EPR and H_2 -TPR results. In combination with the non-framework Al centered at -36.5 ppm (Figure 10), CuAlO_x species came from the reactions with Cu_xO , CuO , and non-framework Al.

The results above reveal that the reduced Cu^{2+} ions caused by Na introducing transformed to other copper species (Cu_xO , CuO , and CuAlO_x species). To further prove this variation regulation, NH_3 oxidation over all catalysts are shown in Figure 11. Olsson and Lerstner [33,34] have pointed out that NH_3 oxidation at low temperature (≤ 300 °C) occurs on Cu^{2+} ions in 6 MR, while $[\text{Cu}(\text{OH})]^+$ in 8 MR and copper oxide species were responsible for NH_3 oxidation at a higher temperature (> 400 °C). At 300 °C, the NH_3 conversion of Na impregnated catalysts was lower than that of F-Cu and NH_3 conversion showed a decreasing trend with increasing Na contents, which confirmed the decreasing amounts of Cu^{2+} ions in 6 MR. When the temperature was higher than 400 °C, Cu_xO and CuO improved the NH_3 conversion on all impregnated catalysts, because the NH_3 oxidation reaction could easily occur on copper oxide species. Based on all the conclusions above, the deactivation mechanism of Na on Cu/SSZ-13 is proposed in Scheme 1.

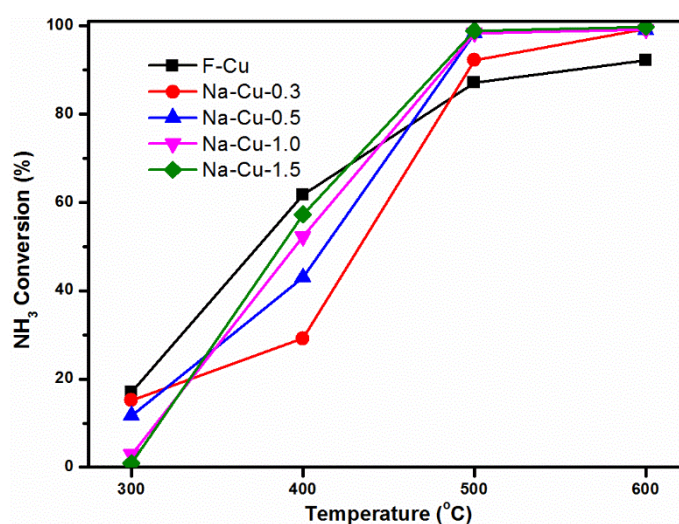
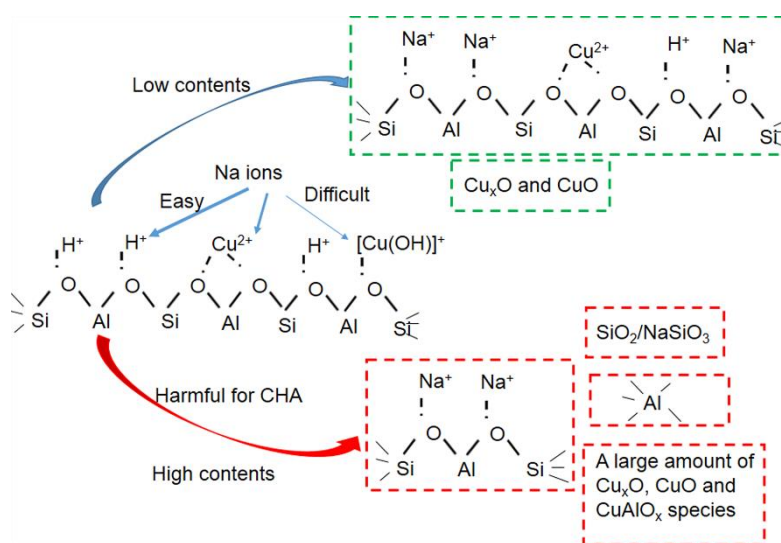


Figure 11. NH_3 oxidation results of fresh and Na-impregnated catalysts. The reaction was carried out with a feed containing 500 ppm NH_3 , 10% O_2 , 3% H_2O , balance N_2 , and with GHSV = $80,000 \text{ h}^{-1}$.



Scheme 1. Nature of the Na ions on Cu/SSZ-13 catalysts.

3.3. Effect of Na on the NH₃-SCR Reaction

Based on the conclusions above, the impregnated Na's impact on NH₃-SCR reaction (at low and high temperature) can be addressed. According to E_a measurement results, four catalysts—F-Cu, Na-Cu-0.3, Na-Cu-0.5, and Na-Cu-1.0—had the same E_a value, suggesting the same NH₃-SCR reaction mechanism. Therefore, as shown in Figure 12, the turnover frequencies (TOFs) of these four catalysts were calculated based on their reaction rate and the number of Cu²⁺ ions from the EPR results (Figure 5). The identical TOFs for F-Cu, Na-Cu-0.3, Na-Cu-0.5, and Na-Cu-1.0 illustrate that the Cu²⁺ ions were the active sites for NH₃-SCR reaction at kinetic temperature region and the existing Na ions could not influence the nature of the remaining Cu²⁺ ions that were not occupied by Na⁺.

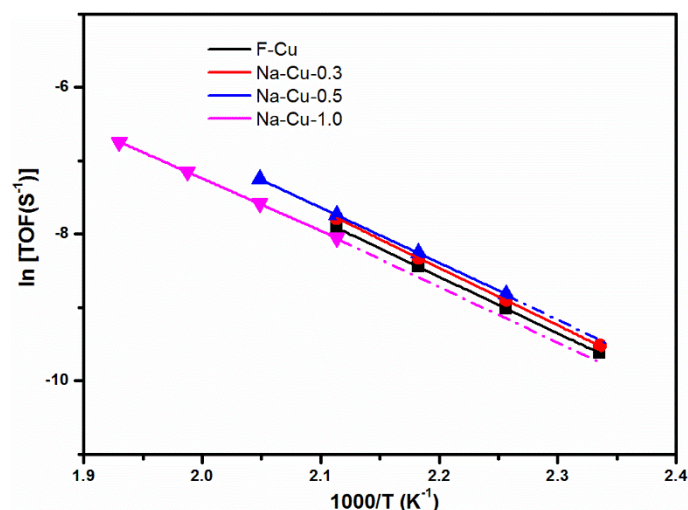


Figure 12. TOFs results of fresh and Na-impregnated catalysts.

It is also worth noting that Na-Cu-1.5 showed a different E_a value compared with others, demonstrating a different rate-determining step occurred for Na-Cu-1.5. Recently, Paolucci [35] found that NH₃-SCR reactions become second-order in low Cu contents when Cu/Al is lower than 0.1. They also pointed out that NH₃-solvated Cu could migrate in the CHA structure to form a Cu dimer species and the formation of Cu-dimer was the rate-determining step. According to our H₂-TPR and ex situ DRIFTS results of Na-Cu-1.5, only Cu²⁺ in 8 MR remained, and the amounts of Cu²⁺ ions should be less than half of the content of Cu²⁺ ions on Na-Cu-1.0. Based on the stoichiometry of SSZ-13 (H_{2.77}Al_{2.77}Si_{33.23}O₇₂), the ion-exchange level (Cu/Al) of Na-Cu-1.5 was lower than 0.03. Therefore, it is reasonable to believe that the formation of the Cu-dimer species was the rate-determining step on this catalysts. Moreover, Na occupied all Brønsted acid sites, as shown in our NH₃-TPR results (Figure 2), and the migration of solvated Cu to Cu-dimer species became difficult due to the larger steric hindrance of Na ions. Besides that, the pore diffusion limitations caused by the damage of CHA structure and formation of another phase also contributed to the lower E_a value, which agreed well with the report by Chen [23], who found the high content of phosphorus impregnated Cu/SSZ-13 showed lower E_a compared with the fresh one. In their study, the damage of zeolitic structure, the pore diffusion limitations, the formation of new Cu copper species, and the reduction in the number of acid sites and Cu²⁺ ions could explain the lower E_a value.

When the temperature was higher than that of the kinetic region, it clearly showed that the NO_x conversion became lower when Na metal loadings increased. Since isolated Cu²⁺ monomers were the active sites for NH₃-SCR activity at high temperatures [1] and a higher amount of Brønsted acid sites is beneficial to SCR activity [10], Na-impregnated catalysts with a gradual decrease of Cu²⁺ contents and Brønsted acid sites had an inferior SCR performance. Moreover, the continuous increase of Cu_xO and CuO amounts on Na-impregnated catalysts had a higher NH₃ oxidation ability, as shown in Figure 11, and this competitive reaction also helped to explain the low SCR activity at high temperatures.

4. Materials and Methods

4.1. Materials

In this study, Cu/SSZ-13 samples with Si/Al = 12 were prepared using a two-step solution ion exchange method. First, Na/SSZ-13 with Si/Al = 12 were synthesized using a hydrothermal method and the detailed synthesized processes can be found in Reference [27]. Briefly, the synthesis gel composition was listed as follows: 1 SiO₂: 0.04 Al₂O₃: 0.025 Na₂O: 0.1 SDA: 20 H₂O. Before the ion exchange process, the obtained powder was dried in an oven at 100 °C for 12 h and calcined in a muffle furnace with air at 650 °C for 8 h to remove the template agent. A proportion of 1.91% Cu/SSZ-13 was prepared via exchanging Na/SSZ-13 in a 1 M (NH₄)₂SO₄ solution at 80 °C for 4 h and 0.5 M Cu(NO₃)₂ at 80 °C for 1 h, respectively. Finally, the samples were calcined at 550 °C for 6 h in a muffle furnace to obtain Cu/SSZ-13.

In order to probe the nature of Na ions on Cu/SSZ-13 catalysts, four different Na loading Cu/SSZ-13 catalysts of 0.3, 0.5, 1.0, and 1.5 mmol/g were prepared using an incipient wetness impregnation method. Briefly, 4 g of fresh Cu/SSZ-13 was put into the required amount solution of NaNO₃ and the obtained slurry was dried at 100 °C for 24 h. Then, the catalysts were calcined in a muffle furnace with air at 550 °C for 5 h. Finally, all Na impregnated and reference (Cu/SSZ-13) catalysts were treated at 600 °C for 16 h in 10% H₂O/air. Their corresponding catalyst nomenclatures is shown in Table 1. The reference catalyst was named “F-Cu” and the impregnated catalysts were denoted as “Na-Cu-X,” where X stands for metal loading.

4.2. Methods

The compositions of Cu/SSZ-13 catalysts were determined using ICP-AES.

The BET surface areas of Cu/SSZ-13s were measured using Brunauer–Emmett–Teller measurements (Norcross, GA, USA) after dehydration of the catalysts at 300 °C for 24 h under vacuum.

The XRD spectra were collected using an X' Pert Pro diffractometer with nickel-filtered Cu K α radiation ($\lambda = 1.5418$ Å), operating at 40 kV and 40 mA in the range of 5–50° with a step size of 0.01°.

The structural damage mechanism was investigated using ²⁹Si and ²⁷Al NMR measurements. ²⁹Si and ²⁷Al NMR measurements were tested on a Varian Infinity plus 300 WB spectrometer at resonance frequencies of 59.57 and 78.13 MHz, respectively, with sample-spinning rates of 4 kHz for ²⁹Si and 8 kHz for ²⁷Al. Tetramethylsilane (TMS) and Al(NO₃)₃ aqueous solutions were used as a chemical reference for ²⁹Si and ²⁷Al NMR spectroscopy, respectively.

DRIFTS tests were performed using Nicolet 6700 FTIR (Waltham, MA, USA). KBr was chosen as the standard substance to make the background for ex situ tests. For CO₂-DRIFTS, the samples were initially treated in 5% O₂/N₂ at 500 °C for 30 min and then cooled to 50 °C in N₂. The background spectrum was collected first when the temperature became stable, then the sample was purged in 1% CO₂/N₂ for 15 min and N₂ for only 30 min, and the spectra were collected.

NH₃-TPD experiments were performed to reveal the acidity of catalysts. The catalysts/supports were dehydrated at 250 °C for 30 min in 5% O₂/N₂, and then cooled to 100 °C in N₂. The samples were purged using 500 ppm NH₃/N₂ at 100 °C until NH₃ concentration was stable. Then, the samples were purged with N₂ to remove any weakly absorbed NH₃ at 100 °C. When the NH₃ concentration was lower than 10 ppm, the samples were heated from 100 °C to 550 °C at a ramping rate of 10 °C/min.

The overall changing tendency of active sites was measured by EPR at –150 °C when hydrated Cu/SSZ-13s were used and quantitative results were obtained using CuSO₄·5H₂O as a reference.

H₂-TPR were further used to probe the copper species variation. Prior to reduction, the samples (100 mg) were first treated at 250 °C under 5% O₂/N₂. Then, the samples were cooled down to room temperature, followed by purging in N₂. Finally, the samples were measured in a flow of 5% H₂/N₂ (10 mL/min⁻¹) from 30 °C to 900 °C at a ramping rate of 10 °C/min.

Copper oxide species were particularly tested using Shimadzu UV-3600 spectrometer (Kyoto, Japan) equipped with BaSO₄ as the reference.

NH₃-SCR and kinetic tests were performed on all catalysts. The detailed description of the experimental process and calculation about NO_x conversion, NH₃-SCR reaction rates, and turnover frequency (TOF) can be found in our previous studies [11,36]. NH₃ oxidation measurements were also performed to clearly explain the NH₃-SCR activity.

5. Conclusions

The Na effect on a Cu/SSZ-13 catalyst after mild hydrothermal aging has been investigated with respect to different Na loadings. The main conclusions of this study are listed below:

1. The impregnated Na exchanged with Brönsted acid sites and Cu²⁺ ions as Si-O(Na⁺)-Al. The Na intakes declined with the number of acid sites, including Brönsted acid sites and Cu²⁺ ions. The reduction degree of the number of Brönsted acid sites were greater than that of Cu²⁺ ions contents.
2. Except for sample with highest Na loading (1.5 mmol/g), all Na-impregnated catalysts remained as two types of Cu²⁺ ions and the overall amounts of Cu²⁺ ions declined with Na and increase in contents. Na-Cu-1.5 only contained Cu²⁺ ions in 8 MR and it had the lowest amounts of Cu²⁺.
3. The Na introduced damage to the framework of catalysts and formed SiO₂/NaSiO₃ and amorphous species when the contents of Na ≥ 1.0 mmol/g, as confirmed using XRD, BET, and NMR results.
4. The reduced Cu²⁺ ions changed into other copper species, Cu_xO, CuO, and CuAlO_x species. Furthermore, CuAlO_x species were only generated on Na-Cu-1.5 catalyst.
5. For Na-impregnated catalysts, the loss of Cu²⁺ contents contributed to the inferior SCR activity at low temperatures, while at high temperatures, the reduction in the number of acid sites and Cu²⁺ ions as well as CuO_x species formation lead to low SCR performance.

Supplementary Materials: The following are available online at <http://www.mdpi.com/2073-4344/8/12/593/s1>, Figure S1: DRIFTS spectra of NH₃-TPD over Cu/SSZ-13 catalysts, Figure S2: XRD results of Na-Cu-0.3 after hydrothermal aging at 750 °C for 16 h.

Author Contributions: Conceptualization, C.W.; Formal analysis, J.W. (Jianqiang Wang); Funding acquisition, J.W. (Jun Wang), M.S. and C.W.; Investigation, Z.C., Z.W., X.L., and X.K.; Methodology, J.W. (Jun Wang) and M.S.; Project administration, J.W. (Jun Wang); Resources, M.S.; Supervision, C.W. and M.S.; Validation, J.W. (Jianqiang Wang), W.Y. and X.K.; Visualization, C.W.; Writing—review and editing, C.W.

Funding: This research was funded by National Key Research and Development program, grant number 2017YFC0211302; National Natural Science Foundation of China, grant number 21676195; Science Fund of State Key Laboratory of Engine Reliability, grant number skler-201714; and the State Key Laboratory of Advanced Technology for Comprehensive Utilization of Platinum Metals, grant number SKL-SPM-2018017.

Conflicts of Interest: The authors declare no conflict of interest.

References

1. Gao, F.; Walter, E.D.; Kollar, M.; Wang, Y.; Szanyi, J.; Peden, C.H.F. Understanding ammonia selective catalytic reduction kinetics over Cu/SSZ-13 from motion of the Cu ions. *J. Catal.* **2014**, *319*, 1–14. [[CrossRef](#)]
2. Han, S.; Cheng, J.; Zheng, C.; Ye, Q.; Cheng, S.; Kang, T.; Dai, H. Effect of Si/Al ratio on catalytic performance of hydrothermally aged Cu-SSZ-13 for the NH₃-SCR of NO in simulated diesel exhaust. *Appl. Surf. Sci.* **2017**, *419*, 382–392. [[CrossRef](#)]
3. Song, J.; Wang, Y.; Walter, E.D.; Washton, N.M.; Mei, D.; Kovarik, L.; Engelhard, M.H.; Proding, S.; Wang, Y.; Peden, C.H.F.; et al. Toward Rational Design of Cu/SSZ-13 Selective Catalytic Reduction Catalysts: Implications from Atomic-Level Understanding of Hydrothermal Stability. *ACS Catal.* **2017**, *7*, 8214–8227. [[CrossRef](#)]
4. Leistner, K.; Kumar, A.; Kamasamudram, K.; Olsson, L. Mechanistic study of hydrothermally aged Cu/SSZ-13 catalysts for ammonia-SCR. *Catal. Today* **2018**, *307*, 55–64. [[CrossRef](#)]
5. Luo, J.; Gao, F.; Kamasamudram, K.; Currier, N.; Peden, C.H.F.; Yezerets, A. New insights into Cu/SSZ-13 SCR catalyst acidity. Part I: Nature of acidic sites probed by NH₃ titration. *J. Catal.* **2017**, *348*, 291–299. [[CrossRef](#)]

6. Fan, C.; Chen, Z.; Pang, L.; Ming, S.; Zhang, X.; Albert, K.B.; Liu, P.; Chen, H.; Li, T. The influence of Si/Al ratio on the catalytic property and hydrothermal stability of Cu-SSZ-13 catalysts for NH₃-SCR. *Appl. Catal. A Gen.* **2018**, *550*, 256–265. [[CrossRef](#)]
7. Gargiulo, N.; Caputo, D.; Totarella, G.; Lisi, L.; Cimino, S. Me-ZSM-5 monolith foams for the NH₃-SCR of NO. *Catal. Today* **2018**, *304*, 112–118. [[CrossRef](#)]
8. Lin, Q.; Liu, J.; Liu, S.; Xu, S.; Lin, C.; Feng, X.; Wang, Y.; Xu, H.; Chen, Y. Barium-promoted hydrothermal stability of monolithic Cu/BEA catalyst for NH₃-SCR. *Dalton Trans.* **2018**, *47*, 15038–15048. [[CrossRef](#)] [[PubMed](#)]
9. Ma, J.; Si, Z.; Weng, D.; Wu, X.; Ma, Y. Potassium poisoning on Cu-SAPO-34 catalyst for selective catalytic reduction of NO_x with ammonia. *Chem. Eng. J.* **2015**, *267*, 191–200. [[CrossRef](#)]
10. Wang, L.; Li, W.; Schmiege, S.J.; Weng, D. Role of Brønsted acidity in NH₃ selective catalytic reduction reaction on Cu/SAPO-34 catalysts. *J. Catal.* **2015**, *324*, 98–106. [[CrossRef](#)]
11. Wang, C.; Wang, C.; Wang, J.; Wang, J.; Shen, M.; Li, W. Effects of Na(+) on Cu/SAPO-34 for ammonia selective catalytic reduction. *J. Environ. Sci.* **2018**, *70*, 20–28. [[CrossRef](#)] [[PubMed](#)]
12. Gao, F.; Wang, Y.; Washton, N.M.; Kollár, M.; Szanyi, J.; Peden, C.H.F. Effects of Alkali and Alkaline Earth Cocations on the Activity and Hydrothermal Stability of Cu/SSZ-13 NH₃-SCR Catalysts. *ACS Catal.* **2015**, *5*, 6780–6791. [[CrossRef](#)]
13. Zhao, Z.; Yu, R.; Zhao, R.; Shi, C.; Gies, H.; Xiao, F.-S.; De Vos, D.; Yokoi, T.; Bao, X.; Kolb, U.; et al. Cu-exchanged Al-rich SSZ-13 zeolite from organotemplate-free synthesis as NH₃-SCR catalyst: Effects of Na⁺ ions on the activity and hydrothermal stability. *Appl. Catal. B Environ.* **2017**, *217*, 421–428. [[CrossRef](#)]
14. Xie, L.; Liu, F.; Shi, X.; Xiao, F.-S.; He, H. Effects of post-treatment method and Na co-cation on the hydrothermal stability of Cu-SSZ-13 catalyst for the selective catalytic reduction of NO_x with NH₃. *Appl. Catal. B Environ.* **2015**, *179*, 206–212. [[CrossRef](#)]
15. Fan, C.; Chen, Z.; Pang, L.; Ming, S.; Dong, C.; Brou Albert, K.; Liu, P.; Wang, J.; Zhu, D.; Chen, H.; et al. Steam and alkali resistant Cu-SSZ-13 catalyst for the selective catalytic reduction of NO_x in diesel exhaust. *Chem. Eng. J.* **2018**, *334*, 344–354. [[CrossRef](#)]
16. Liu, Q.; Fu, Z.; Ma, L.; Niu, H.; Liu, C.; Li, J.; Zhang, Z. MnO_x-CeO₂ supported on Cu-SSZ-13: A novel SCR catalyst in a wide temperature range. *Appl. Catal. A Gen.* **2017**, *547*, 146–154. [[CrossRef](#)]
17. Wang, J.; Peng, Z.; Qiao, H.; Yu, H.; Hu, Y.; Chang, L.; Bao, W. Cerium-Stabilized Cu-SSZ-13 Catalyst for the Catalytic Removal of NO_x by NH₃. *Ind. Eng. Chem. Res.* **2016**, *55*, 1174–1182. [[CrossRef](#)]
18. Tang, J.; Xu, M.; Yu, T.; Ma, H.; Shen, M.; Wang, J. Catalytic deactivation mechanism research over Cu/SAPO-34 catalysts for NH₃-SCR (II): The impact of copper loading. *Chem. Eng. Sci.* **2017**, *168*, 414–422. [[CrossRef](#)]
19. Wang, D.; Jangjou, Y.; Liu, Y.; Sharma, M.K.; Luo, J.; Li, J.; Kamasamudram, K.; Epling, W.S. A comparison of hydrothermal aging effects on NH₃-SCR of NO_x over Cu-SSZ-13 and Cu-SAPO-34 catalysts. *Appl. Catal. B Environ.* **2015**, *165*, 438–445. [[CrossRef](#)]
20. Luo, J.; Wang, D.; Kumar, A.; Li, J.; Kamasamudram, K.; Currier, N.; Yezerets, A. Identification of two types of Cu sites in Cu/SSZ-13 and their unique responses to hydrothermal aging and sulfur poisoning. *Catal. Today* **2016**, *267*, 3–9. [[CrossRef](#)]
21. Kwak, J.H.; Varga, T.; Peden, C.H.F.; Gao, F.; Hanson, J.C.; Szanyi, J. Following the movement of Cu ions in a SSZ-13 zeolite during dehydration, reduction and adsorption: A combined in situ TP-XRD, XANES/DRIFTS study. *J. Catal.* **2014**, *314*, 83–93. [[CrossRef](#)]
22. Godiksen, A.; Stappen, F.N.; Vennestrøm, P.N.R.; Giordanino, F.; Rasmussen, S.B.; Lundegaard, L.F.; Mossin, S. Coordination Environment of Copper Sites in Cu-CHA Zeolite Investigated by Electron Paramagnetic Resonance. *J. Phys. Chem. C* **2014**, *118*, 23126–23138. [[CrossRef](#)]
23. Chen, Z.; Fan, C.; Pang, L.; Ming, S.; Liu, P.; Li, T. The influence of phosphorus on the catalytic properties, durability, sulfur resistance and kinetics of Cu-SSZ-13 for NO_x reduction by NH₃-SCR. *Appl. Catal. B Environ.* **2018**, *237*, 116–127. [[CrossRef](#)]
24. Kim, Y.J.; Lee, J.K.; Min, K.M.; Hong, S.B.; Nam, I.-S.; Cho, B.K. Hydrothermal stability of CuSSZ13 for reducing NO_x by NH₃. *J. Catal.* **2014**, *311*, 447–457. [[CrossRef](#)]
25. Gao, F.; Walter, E.D.; Washton, N.M.; Szanyi, J.; Peden, C.H.F. Synthesis and evaluation of Cu/SAPO-34 catalysts for NH₃-SCR 2: Solid-state ion exchange and one-pot synthesis. *Appl. Catal. B Environ.* **2015**, *162*, 501–514. [[CrossRef](#)]

26. Zhang, T.; Qiu, F.; Chang, H.; Li, X.; Li, J. Identification of active sites and reaction mechanism on low-temperature SCR activity over Cu-SSZ-13 catalysts prepared by different methods. *Catal. Sci. Technol.* **2016**, *6*, 6294–6304. [[CrossRef](#)]
27. Gao, F.; Washton, N.M.; Wang, Y.; Kollár, M.; Szanyi, J.; Peden, C.H.F. Effects of Si/Al ratio on Cu/SSZ-13 NH₃-SCR catalysts: Implications for the active Cu species and the roles of Brønsted acidity. *J. Catal.* **2015**, *331*, 25–38. [[CrossRef](#)]
28. Zhang, T.; Qiu, F.; Li, J. Design and synthesis of core-shell structured meso-Cu-SSZ-13@mesoporous aluminosilicate catalyst for SCR of NO_x with NH₃: Enhancement of activity, hydrothermal stability and propene poisoning resistance. *Appl. Catal. B Environ.* **2016**, *195*, 48–58. [[CrossRef](#)]
29. Wang, J.; Peng, Z.; Qiao, H.; Han, L.; Bao, W.; Chang, L.; Feng, G.; Liu, W. Influence of aging on in situ hydrothermally synthesized Cu-SSZ-13 catalyst for NH₃-SCR reaction. *RSC Adv.* **2014**, *4*, 42403–42411. [[CrossRef](#)]
30. Li, J.; Wilken, N.; Kamasamudram, K.; Currier, N.W.; Olsson, L.; Yezerets, A. Characterization of Active Species in Cu-Beta Zeolite by Temperature-Programmed Reduction Mass Spectrometry (TPR-MS). *Top. Catal.* **2013**, *56*, 201–204. [[CrossRef](#)]
31. Leistner, K.; Xie, K.; Kumar, A.; Kamasamudram, K.; Olsson, L. Ammonia Desorption Peaks Can Be Assigned to Different Copper Sites in Cu/SSZ-13. *Catal. Lett.* **2017**, *147*, 1882–1890. [[CrossRef](#)]
32. Wang, J.; Fan, D.; Yu, T.; Wang, J.; Hao, T.; Hu, X.; Shen, M.; Li, W. Improvement of low-temperature hydrothermal stability of Cu/SAPO-34 catalysts by Cu²⁺ species. *J. Catal.* **2015**, *322*, 84–90. [[CrossRef](#)]
33. Xie, K.; Leistner, K.; Wijayanti, K.; Kumar, A.; Kamasamudram, K.; Olsson, L. Influence of phosphorus on Cu-SSZ-13 for selective catalytic reduction of NO_x by ammonia. *Catal. Today* **2017**, *297*, 46–52. [[CrossRef](#)]
34. Leistner, K.; Mihai, O.; Wijayanti, K.; Kumar, A.; Kamasamudram, K.; Currier, N.W.; Yezerets, A.; Olsson, L. Comparison of Cu/BEA, Cu/SSZ-13 and Cu/SAPO-34 for ammonia-SCR reactions. *Catal. Today* **2015**, *258*, 49–55. [[CrossRef](#)]
35. Paolucci, C.; Khurana, I.; Parekh, A.A.; Li, S.; Shih, A.J.; Li, H.; di Iorio, J.R.; Albarracín-Caballero, J.D.; Yezerets, A.; Miller, J.T.; et al. Dynamic multinuclear sites formed by mobilized copper ions in NO_x selective catalytic reduction. *Science* **2017**, *357*, 898–903. [[CrossRef](#)] [[PubMed](#)]
36. Wang, C.; Wang, J.; Wang, J.; Yu, T.; Shen, M.; Wang, W.; Li, W. The effect of sulfate species on the activity of NH₃-SCR over Cu/SAPO-34. *Appl. Catal. B Environ.* **2017**, *204*, 239–249. [[CrossRef](#)]



© 2018 by the authors. Licensee MDPI, Basel, Switzerland. This article is an open access article distributed under the terms and conditions of the Creative Commons Attribution (CC BY) license (<http://creativecommons.org/licenses/by/4.0/>).